Starting Homoclinic Tangencies near 1 : 1 Resonances

Joseph Páez Chávez*

Instituto de Ciencias Matemáticas,
Escuela Superior Politécnica del Litoral,
Km. 30.5 Vía Perimetral, P.O. Box 09-01-5863
Guayaquil, Ecuador
jpaez@espol.edu.ec

April 9, 2010

Abstract

We construct a theory-based numerical method for starting the continuation of homoclinic tangencies near 1 : 1 resonances, for systems with arbitrary dimension ≥ 2. The core of the method is numerical center manifold reduction and flow approximation. The reduction is implemented by means of the homological equation. The starting procedure is applied in numerical examples.

1 Introduction

A typical problem in the numerical analysis of homoclinic orbits is the choice of an appropriate initial guess that could lead us, via e.g. Newton iterations, to the homoclinic connection we want to analyze. In our case we have a well-posed problem given in terms of a suitably defined operator (see Section 2), whose solutions correspond to the numerical approximation of the homoclinic tangencies we are interested in. Thus we will construct a theory-based starting procedure, by means of which we can obtain an "educated" initial guess of the solution of the underlying well-posed problem.

What is commonly done is to set a first approximating orbit to

$$(\ldots, \xi, \ldots, \xi, x_1, \ldots, x_r, \xi, \ldots, \xi, \ldots),$$

where ξ represents an equilibrium point and x_i, $i = 1, \ldots, r$, $r \in \mathbb{N}$ are, basically, randomly chosen vectors on the state space. This method is successfully applied, e.g., in [14, 15].

*Supported by CRC 701 'Spectral Structures and Topological Methods in Mathematics', Bielefeld University.

This is of course a purely trial-and-error-based method, where the user relies entirely on "luck" or brute force. Therefore, the user has essentially no control over the outcome of the Newton iterations, and it can easily happens that a spurious solution is obtained, which is a significant disadvantage.

Another approach consists of finding the intersections of the stable and unstable manifolds and using these intersections as an initial guess (see Figure 2.2). By doing this, a transversal homoclinic orbit is generically obtained via Newton iterations. Once this is done, the transversal orbit is continued with respect to one parameter until a turning point of the defining system is found. Finally, this turning point is used as initial guess of the homoclinic tangency (cf. [12]). However, the disadvantage of this method is that in order to find an approximation of the transversal orbits, the stable and unstable manifolds of the system need to be numerically approximated, which is itself a problem. Furthermore, this technique is reasonably applicable only when working with planar systems. Moreover, since the systems we deal with depend on parameters, we have to at least approximately know at which parameter-values the homoclinic connection occurs, so that the manifolds intersect at all.

Thus, our main concern throughout this article will be the construction of a theory-based method that allows us to start the continuation of tangential homoclinic orbits near $1:1$ resonances, with no restriction of the dimension of the system. The basic idea is the following. We assume we are given a parameter-dependent, discrete-time dynamical system which undergoes a $1:1$ resonance at the origin. By means of the homological equation (cf. Section 3), we perform a quantitative center manifold reduction, so that, up to a certain order, we can transform orbits of the normal form to orbits of the original system. Then we approximate the normal form by the 1-flow of a vector field which undergoes a generic Bogdanov-Takens singularity at the origin (cf. Lemma 2.5). By doing this, we merely transform the original discrete-time problem into a continuous one. Consequently, we just need to apply any of the known techniques for starting the continuation of homoclinic orbits near a Bogdanov-Takens point. In our implementation we will apply the method described in Section 4 (cf. [3]). Then we need to transform the thus obtained approximating orbit back to the normal form, via Lemma 2.5, and finally to the original system, by means of the quantitative center manifold reduction. Once this is achieved, the so obtained initial guess can be used for starting the Newton iterations in order to obtain the approximation of a homoclinic tangency, and thereby we will be able to quantitatively explore the homoclinic structure in various interesting examples, since homoclinic orbits are one of the most fascinating objects of study in the theory of dynamical systems, because their presence leads to nontrivial dynamics.

2 Basic Setup

Let $f(\cdot,\alpha)$, $f \in C^k(\mathbb{R}^N \times \mathbb{R}^p, \mathbb{R}^N)$, $k \geq 1$, be a diffeomorphism for all $\alpha \in \mathbb{R}^p$. Throughout this section we consider the discrete-time system

$$x \mapsto f(x,\alpha). \tag{2.1}$$

Definition 2.1. *Suppose that $\xi \in \mathbb{R}^N$ is a hyperbolic equilibrium of (2.1) at $\alpha = \alpha_0$. An orbit $x_{\mathbb{Z}} \in \left(\mathbb{R}^N\right)^{\mathbb{Z}}$ of (2.1) is referred to as homoclinic with respect to ξ (in short homoclinic) if*

$$\lim_{n\to\pm\infty} x_n = \xi.$$

The main objects of study of the present work are tangential homoclinic orbits, which are formally defined as follows:

Definition 2.2. *A homoclinic orbit $x_{\mathbb{Z}} \in \left(\mathbb{R}^N\right)^{\mathbb{Z}}$ of (2.1) is referred to as r-tangential, r some nonnegative integer, if the homogeneous difference equation*

$$u_{n+1} = f_x(x_n, \alpha_0)u_n, \quad n \in \mathbb{Z}$$

has r linearly independent bounded solutions. Furthermore, an r-tangential homoclinic orbit $x_{\mathbb{Z}} \in \left(\mathbb{R}^N\right)^{\mathbb{Z}}$ is called nondegenerate with respect to the parameter $\alpha \in \mathbb{R}^p$, if $p = r$ and every bounded solution $(u_{\mathbb{Z}}, \mu) \in \left(\mathbb{R}^N\right)^{\mathbb{Z}} \times \mathbb{R}^p$ of the difference equation

$$u_{n+1} = f_x(x_n, \alpha_0)u_n + f_\alpha(x_n, \alpha_0)\mu, \quad n \in \mathbb{Z}$$

satisfies $\mu = 0$.

In particular we will deal with 1-tangential (in short tangential) and transversal homoclinic orbits (i.e. 0-tangential homoclinic orbits).

Before introducing the already known numerical methods for the computation of homoclinic orbits, it is worth presenting a theorem that characterizes these objects as solutions of a suitably defined operator. In fact, the numerical methods we will work with can be seen as truncated versions of the underlying operator. For this purpose we first need to define some Banach spaces over which the (truncated) operator will act. Let $N_+, N_- \in \mathbb{Z} \cup \{\pm\infty\}$, $N_- < 0 < N_+$. Define the discrete intervals

$$J := [N_-, N_+] \cap \mathbb{Z},$$

and

$$\hat{J} := [N_-, N_+ - 1] \cap \mathbb{Z},$$

if $N_+ < \infty$. Define the space of bounded sequences

$$S_J^N := \left\{ x_J \in \left(\mathbb{R}^N\right)^J : \sup_{n\in J} ||x_n|| < \infty \right\},$$

where $||\cdot||$ is any norm in $\mathbb{R}^N$. It is well known that S_J^N equipped with the norm

$$||x_J||_\infty := \sup_{n\in J} ||x_n||,$$

$x_J \in S_J^N$, is a Banach space. Furthermore we allow $J = \mathbb{Z}$, and thus we obtain the Banach space $S_{\mathbb{Z}}^N$. With this basic setup we can now define the operator

$$\Gamma : \begin{array}{rcl} S_{\mathbb{Z}}^N \times \mathbb{R}^p & \to & S_{\mathbb{Z}}^N \\ (x_{\mathbb{Z}}, \alpha) & \mapsto & (x_{n+1} - f(x_n, \alpha))_{n\in\mathbb{Z}} \end{array}.$$

By means of this operator, a homoclinic orbit (in the sense of Definition 2.1) can be regarded as the solution of the infinite boundary value problem

$$\begin{cases} \Gamma(x_{\mathbb{Z}}, \alpha_0) = 0, \\ \lim_{n\to\pm\infty} x_n = \xi. \end{cases} \tag{2.2}$$

The following theorem characterizes tangential and transversal homoclinic orbits in terms of the operator Γ:

Theorem 2.3. *Let $p = 1$ and $x_{\mathbb{Z}} \in S^N_{\mathbb{Z}}$ be a homoclinic orbit of (2.1) at $\alpha = \alpha_0$. Then, the following assertions hold:*

(i) $x_{\mathbb{Z}}$ is transversal, if and only if $x_{\mathbb{Z}}$ is a regular zero of $\Gamma(\cdot, \alpha_0)$,

(ii) $x_{\mathbb{Z}}$ is tangential and nondegenerate with respect to α, if and only if $(x_{\mathbb{Z}}, \alpha_0)$ is a turning point of Γ in α.

Proof. See [14, Theorem 3.4] and [15, Proposition 2.1.3]. □

Now that we have formally introduced the objects we want to work with, we can start with the numerical part of this section, i.e., the numerical computation of transversal and tangential homoclinic orbits. Let us then begin with the approximation of transversal homoclinic orbits. The main idea is to replace the infinite boundary value problem (2.2) by a finite, truncated one. To do so, define the operator

$$\hat{\Gamma}: \begin{array}{rcl} S^N_J \times \mathbb{R}^p & \to & S^N_J \\ (x_J, \alpha) & \mapsto & \left((x_{n+1} - f(x_n, \alpha))_{n\in\hat{J}}, b(x_{N_-}, x_{N_+}, \alpha)\right) \end{array},$$

where $b : \mathbb{R}^{2N} \times \mathbb{R}^p \to \mathbb{R}^N$ represents a boundary condition. In particular we will consider periodic and projection boundary conditions. Let $\bar{x}_{\mathbb{Z}} \in S^N_{\mathbb{Z}}$ be a transversal homoclinic orbit of (2.1) at $\alpha = \alpha_0$ with respect to the equilibrium $\xi \in \mathbb{R}^N$. Let $-N_-, N_+$ be sufficiently large. Then, under certain assumptions, the operator $\hat{\Gamma}(\cdot, \alpha_0)$ has a unique zero $x_J \in S^N_J$ close to $\bar{x}|_J$, and the following estimate holds (cf. [15, Theorem 3.1.2])

$$||\bar{x}|_J - x_J||_\infty \leq C(||\bar{x}_{N_-} - \xi||^s + ||\bar{x}_{N_+} - \xi||^s), \tag{2.3}$$

where C is a positive constant, and $s = 1, 2$, provided b is a periodic, projection boundary condition, respectively.

As for the numerical computation of tangential homoclinic orbits, Theorem 2.3 allows us to intuitively deduce that tangential homoclinic orbits can be approximated by turning points of the operator $\hat{\Gamma}$, with $p = 1$ (see [15, Chapter 7] for a rigorous discussion). Thus, we will approximate tangential homoclinic orbits by zeroes of the following operator

$$\hat{\Upsilon}: \begin{array}{rcl} S^N_J \times S^N_J \times \mathbb{R}^p & \to & S^N_J \times S^N_J \times \mathbb{R} \\ (x_J, u_J, \alpha) & \mapsto & \begin{pmatrix} \hat{\Gamma}(x_J, \alpha) \\ \hat{\Gamma}_{x_J}(x_J, \alpha) u_J \\ \sum_{i=N_-}^{N_+} ||u_i||^2 - 1 \end{pmatrix} \end{array},$$

where $||\cdot||$ represents the Euclidean norm in $\mathbb{R}^N$. In what follows we write $\hat{\Gamma}^T, \hat{\Upsilon}^T$ (resp. $\hat{\Gamma}^P, \hat{\Upsilon}^P$) to denote the use of periodic (resp. projection) boundary conditions. For a detailed discussion about the numerical approximation of transversal, tangential, and other degenerate types of discrete homoclinic orbits we refer to [5, 7, 13, 14, 15].

Let us now focus on a particular case where tangential homoclinic orbits are well known to appear, i.e. near 1 : 1 resonances. In order to formally define this type of singularity, we consider the discrete-time system

$$x \mapsto g(x, \alpha), \tag{2.4}$$

where $g \in C^k(\Omega \times \Lambda, \mathbb{R}^N)$ with open sets $0 \in \Omega \subset \mathbb{R}^N$, $0 \in \Lambda \subset \mathbb{R}^2$, $k \geq 1$ sufficiently large.

Definition 2.4. *A point $(x_0, \alpha_0) \in \Omega \times \Lambda$ is referred to as a nondegenerate 1 : 1 resonance of codimension two (in short $R1_2$ point) of (2.4) if:*

1d $g(x_0, \alpha_0) - x_0 = 0$,

2d *The only Jordan block of $g_x(x_0, \alpha_0)$ corresponding to the eigenvalue 1 is $\begin{pmatrix} 1 & 1 \\ 0 & 1 \end{pmatrix}$, and there are no other eigenvalues on the unit circle,*

3d *$ab \neq 0$, where $a := \frac{1}{2} p_0^T B_g(v_0, v_0)$ and $b := p_1^T B_g(v_0, v_0) + p_0^T B_g(v_0, v_1)$. The bilinear form $B_g(\cdot, \cdot)$ is given by*

$$B_g(v, w) := g_{xx}(x_0, \alpha_0)[v, w] = \sum_{i=1}^{N} \sum_{j=1}^{N} \frac{\partial g(x_0, \alpha_0)}{\partial x_j \partial x_i} v_i w_j,$$

$v, w \in \mathbb{R}^N$ and the vectors $v_0, v_1, p_0, p_1 \in \mathbb{R}^N$ satisfy the set of equations:

$$\begin{array}{ll} (g_x(x_0, \alpha_0) - I_N) v_0 = 0, & (g_x(x_0, \alpha_0) - I_N) v_1 = v_0, \\ (g_x(x_0, \alpha_0) - I_N)^T p_0 = 0, & (g_x(x_0, \alpha_0) - I_N)^T p_1 = p_0, \end{array} \tag{2.5}$$

with $v_0^T p_1 = v_1^T p_0 = 1$ and $v_0^T p_0 = v_1^T p_1 = 0$ (biorthogonality).

Assume system (2.4) to be planar, i.e. $N = 2$, and that it undergoes an $R1_2$ bifurcation at the origin. Then, under certain transversality conditions, there exists a smooth invertible change of coordinates, smoothly depending on parameters, that transforms (2.4) for all sufficiently small $||\alpha||$ into (cf. [17, Lemma 9.7])

$$\begin{pmatrix} \xi_1 \\ \xi_2 \end{pmatrix} \mapsto N_\nu(\xi) := \begin{pmatrix} \xi_1 + \xi_2 \\ \xi_2 + \nu_1 + \nu_2 \xi_2 + A(\nu)\xi_1^2 + B(\nu)\xi_1 \xi_2 \end{pmatrix} + O(||\xi||^3), \tag{2.6}$$

where $A(\cdot)$, $B(\cdot)$ depend smoothly on ν, and $A(0) = a$, $B(0) = b$. The above map is the normal form of the 1 : 1 resonance. Global bifurcations are known to occur in system (2.6), however, the theoretical prediction of such phenomena is rather complicated, if we work with the discrete system. The technique of interpolating a discrete map by a

flow (cf. [9, Takens's Theorem]) is used. The idea is to approximate the discrete system up to a certain order by a 1-flow of a differential equation, and then the already known information about the local bifurcation diagram of the underlying vector field is used for predicting both local, as well as global phenomena that occur in the original discrete system. Thus, in the following lemma N_ν is approximated by a flow(cf. [17, Lemma 9.8]):

Lemma 2.5. *The map* (2.6) *can be represented for all sufficiently small* $||\nu||$ *in the form*

$$N_\nu(\xi) = \varphi_\nu^1(\xi) + O(||\nu||^2) + O(||\xi||^2||\nu||) + O(||\xi||^3),$$

where φ_ν^t *is the flow of a smooth planar system*

$$\dot{\xi} = F(\xi, \nu),$$

with $F(\xi,\nu) := F_0(\nu) + F_1(\xi,\nu) + F_2(\xi)$*, where:*

$$F_0(\nu) := \begin{pmatrix} -\frac{1}{2}\nu_1 \\ \nu_1 \end{pmatrix},$$

$$F_1(\xi,\nu) := \begin{pmatrix} \xi_2 + \left(\frac{1}{3}b - \frac{1}{2}a\right)\nu_1\xi_1 + \left(\left(\frac{1}{5}a - \frac{5}{12}b\right)\nu_1 - \frac{1}{2}\nu_2\right)\xi_2 \\ \left(\frac{2}{3}a - \frac{1}{2}b\right)\nu_1\xi_1 + \left(\left(\frac{1}{2}b - \frac{1}{6}a\right)\nu_1 + \nu_2\right)\xi_2 \end{pmatrix},$$

and

$$F_2(\xi) := \begin{pmatrix} -\frac{1}{2}a\xi_1^2 + \left(\frac{2}{3}a - \frac{1}{2}b\right)\xi_1\xi_2 + \left(\frac{1}{3}b - \frac{1}{6}a\right)\xi_2^2 \\ a\xi_1^2 + (b-a)\xi_1\xi_2 + \left(\frac{1}{6}a - \frac{1}{2}b\right)\xi_2^2 \end{pmatrix}.$$

The dynamics of the above vector field are described by the Bogdanov-Takens theory. Thereby we can predict the existence of a homoclinic structure near the $\mathrm{R1}_2$ singularity. However, some other dynamical phenomena of the original map, e.g. phase-locking Arnold Tongues (cf. [2]), are not present in the approximating flow.

We want to finish this section by pointing out some interesting facts about the homoclinic structure of the normal form of the 1 : 1 resonance. Consider the following system

$$\begin{pmatrix} x_1 \\ x_2 \end{pmatrix} \mapsto \begin{pmatrix} x_1 + x_2 \\ x_2 + \beta + \alpha x_2 + x_1^2 + x_1x_2 \end{pmatrix}, \tag{2.7}$$

where $(x_1, x_2) \in \mathbb{R}^2$, $(\beta, \alpha) \in \mathbb{R}^2$, which is a particular, truncated version of the normal form (2.6). The local bifurcation diagram is shown in Figure 2.1. In this picture, the curves labeled by F, NS correspond to paths of fold, Neimark-Sacker points, respectively. Moreover, the curves labeled by T_1, T_2 represent homoclinic tangencies, which meet, together with NS and F, tangentially at the origin. Between T_1 and T_2 system (2.7) exhibits a transversal homoclinic structure which is limited by the homoclinic tangencies. This structure is schematically represented in Figure 2.2, for $\alpha = \alpha_0$ fixed (see Figure 2.1). In this picture ξ stands for an equilibrium of (2.7), and W_ξ^s, W_ξ^u stand for the stable and unstable manifolds with respect to ξ, respectively.

In Figure 2.1 the distance between T_1 and T_2 is somewhat exaggerated. Actually, this distance is exponentially bounded with respect to one parameter, that is

$$|T_1(\alpha) - T_2(\alpha)| < c_1 e^{-\frac{c_2}{\alpha}},$$

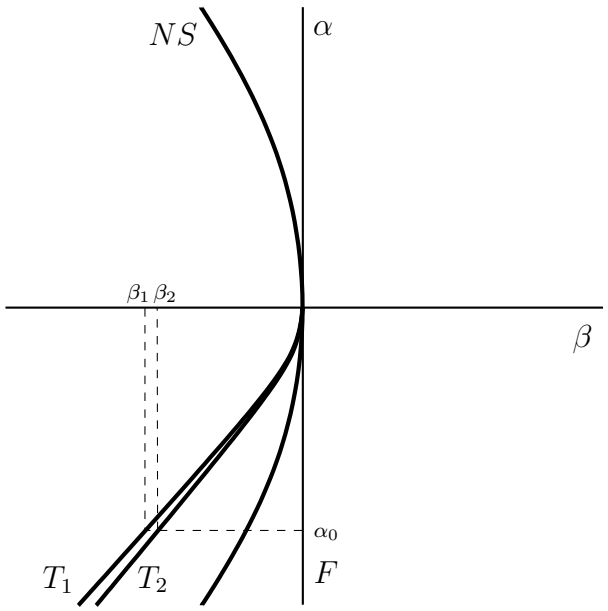

Fig. 2.1: Local bifurcation diagram of system (2.7).

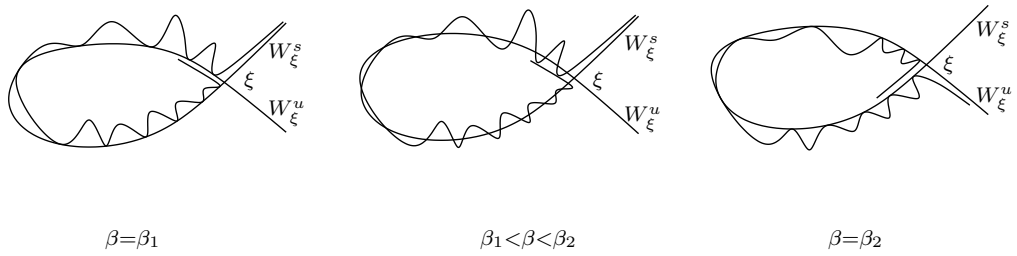

Fig. 2.2: Behavior of stable and unstable manifolds of system (2.7) for $\alpha = \alpha_0$ fixed.

for all $0 < \alpha < c_3$, where $c_{1,2,3} > 0$ are some real constants (cf. [8, 17]). This means that the complete homoclinic structure of system (2.7) survives in an exponentially small sector of the parameter space. This sector is precisely what we want to study numerically.

3 Parameter-dependent Center Manifold Reduction

An important task in the numerical analysis of dynamical systems is the verification of nondegeneracy conditions at bifurcation points, which amounts to computing the coefficients of the normal form of the underlying singularity. In this way, very useful information about the local behavior of a system can be obtained (see e.g. system (2.6)). To accomplish this task, several techniques may be employed, however, the homological-equation-approach has proven to be an efficient and direct method which allows not only the derivation of compact formulae for the computation of normal form coefficients but also the Taylor expansion of the center manifold up to a certain order, in an iterative

manner. The order the center manifold can be expanded up to depends directly on the order of expansion of the underlying normal form. In this section we will use the homological equation for deriving quantitative relations between orbits of the normal form of the $1:1$ resonance and of the original system, where the normal form comes from.

The homological equation has been employed in several applications, e.g., in [17, Section 9.7], [19, Section 3.1 and 3.3.2], [11], [18], for maps, and in [16] for vector fields. The basic idea can be explained as follows. Suppose we are given a discrete-time system

$$x \mapsto f(x, \alpha), \tag{3.1}$$

where $f \in C^k(\Omega_f \times \Lambda_f, \mathbb{R}^N)$, $k \geq 1$ sufficiently large, and $0 \in \Omega_f \subset \mathbb{R}^N$, $0 \in \Lambda_f \subset \mathbb{R}^p$ are open sets. Assume that:

A$_1$ f_x^0 has $N_0 \geq 1$ eigenvalues on the unit circle, and

A$_2$ the system obtained by restriction of (3.1) to a center manifold can be smoothly transformed near the origin to some normal form

$$w \mapsto G(w, \beta), \tag{3.2}$$

where $G : \mathbb{R}^{N_0} \times \mathbb{R}^p \to \mathbb{R}^{N_0}$ is a smooth map.

The shape of G (but not its coefficients) is supposed to be known up to a certain order. Finally, the parameter-dependent center manifold is assumed to be locally parametrized by $(w, \beta) \in \mathbb{R}^{N_0} \times \mathbb{R}^p$, by means of a smooth function

$$Q : \mathbb{R}^{N_0} \times \mathbb{R}^p \to \mathbb{R}^N .$$

Thus, the invariance of the center manifold allows us to presume the existence of a smooth, invertible parameter transformation $K : \mathbb{R}^p \to \mathbb{R}^p$, such that the equation

$$f(Q(w, \beta), K(\beta)) = Q(G(w, \beta), \beta) \tag{3.3}$$

holds locally. The above equation is the so-called homological equation. The use and applications related to this equation are largely explained in the references cited above. A formal statement which actually guarantees the existence of the maps Q, K, so that (3.3) holds, is available in [20]. With these comments about the homological equation we are ready to make use of it in order to perform the numerical center manifold reduction.

Assume that system (3.1), with $p = 2$, has an R1$_2$ point at the origin. Consider the homological equation given in the following way

$$f(H(u, \delta), K(\delta)) = H(G(u, \delta), \delta), \tag{3.4}$$

with:

$$\begin{aligned}
G(u, \delta) &:= \begin{pmatrix} u_1 + u_2 \\ u_2 + \delta_1 + \delta_2 u_2 + a u_1^2 + b u_1 u_2 + O_G((u_1^2 + |u_1 u_2|)||\delta||) \end{pmatrix} + O_G(||u||^3), \\
K(\delta) &:= K_1 \delta + O_K(||\delta||^2), \\
H(u, \delta) &:= \begin{pmatrix} v_0 & v_1 \end{pmatrix} u + D\delta + O_H(||u||^2 + ||u||||\delta|| + ||\delta||^2),
\end{aligned}$$

where $u := (u_1, u_2) \in \mathbb{R}^2$, $\delta := (\delta_1, \delta_2) \in \mathbb{R}^2$, the O_i-symbol, $i = G, K, H$, stands for higher order terms, a, b are the normal form coefficients, and v_0, v_1, p_0, p_1 denote critical right and left generalized eigenvectors of f_x^0, respectively (cf. Definition 2.4). Moreover, $K_1 \in \mathbb{R}^{2,2}$ and $D \in \mathbb{R}^{N,2}$ are quantities to be computed by means of the homological equation. Throughout the computations we consider the Taylor expansion of f

$$f(x, \alpha) = f_x^0 x + f_\alpha^0 \alpha + \frac{1}{2} B(x, x) + O_f(||x||^3 + ||\alpha||^2 + ||x||||\alpha||),$$

where $B(\cdot, \cdot) := f_{xx}^0[\cdot, \cdot]$ (cf. Definition 2.4).

With this basic setup we are ready to perform the numerical center manifold reduction. Replace G, K, H, and f, as explicitly given above, in the homological equation. By doing this, we obtain

$$\begin{aligned} f_x^0 H(u, \delta) + f_\alpha^0 K(\delta) + \frac{1}{2} B(H(u, \delta), H(u, \delta)) + O_f(||H(u, \delta)||^3 + ||K(\delta)||^2 \\ + ||H(u, \delta)||||K(\delta)||) = \begin{pmatrix} v_0 & v_1 \end{pmatrix} G(u, \delta) + D\delta + O_H(||G(u, \delta)||^2 \\ + ||G(u, \delta)||||\delta|| + ||\delta||^2). \end{aligned}$$

By collecting the linear terms in δ of the equation above, we arrive at

$$f_x^0 D\delta + f_\alpha^0 K_1 \delta = \begin{pmatrix} v_1 & 0 \end{pmatrix} \delta + D\delta,$$

and hence it follows

$$(f_x^0 - I_N) D = \begin{pmatrix} v_1 & 0 \end{pmatrix} - f_\alpha^0 K_1. \tag{3.5}$$

Next, the biorthogonality of the critical eigenvectors can be used in order to simplify the above relation. Let us then multiply both sides of the last equation from the left by p_0^T. In this way we obtain the following relation

$$\begin{pmatrix} 1 & 0 \end{pmatrix} = \begin{pmatrix} \beta_1 & \beta_2 \end{pmatrix} K_1, \tag{3.6}$$

where

$$0 \neq \begin{pmatrix} \beta_1 & \beta_2 \end{pmatrix} := p_0^T f_\alpha^0$$

is a transversality condition that must be satisfied. The equation (3.6) does not determine K_1 uniquely, however, a possible choice is readily given by

$$K_1 = \frac{1}{\beta_1^2 + \beta_2^2} \begin{pmatrix} \beta_1 & \sigma\beta_2 \\ \beta_2 & -\sigma\beta_1 \end{pmatrix},$$

where $\sigma \in \{1, -1\}$. Once we have determined K_1, D is immediately obtained from (3.5) by, e.g., bordering techniques (cf. [4]). It is only left to compute the normal form coefficients a, b. These coefficients are well known and given by (cf. [19]):

$$a = \frac{1}{2} p_0^T B(v_0, v_0), \quad b = p_1^T B(v_0, v_0) + p_0^T B(v_0, v_1),$$

(see also Definition 2.4). At this point, an explicit, linear approximation of the center manifold, as well as of the parameter transformation are ready to be used for the computation of orbits of the original system (3.1) from orbits of the normal form.

We want to conclude this section by showing how the homological equation and the numerical center manifold reduction we just derived above will actually help us to construct the starting procedure for the continuation of homoclinic tangencies near an $\mathrm{R1}_2$ point. We have the following:

Proposition 3.1. *Let system* (3.1) *(with $p = 2$) have an $R1_2$ point at the origin. Let $0 \in \Omega_H \subset \mathbb{R}^2$, $0 \in \Lambda_H \subset \mathbb{R}^2$ be open sets, such that the homological equation* (3.4) *holds for all $(u, \delta) \in \Omega_H \times \Lambda_H$. Let $u_{\mathbb{Z}} \in S^2_{\mathbb{Z}}$ be a tangential homoclinic orbit of the normal form $u \mapsto G(u, \delta)$ at $\delta = \delta_0 \in \Lambda_H$, so that $u_i \in \Omega_H$, for all $i \in \mathbb{Z}$. Furthermore, denote by $U_{\mathbb{Z}} \in S^2_{\mathbb{Z}}$ a nontrivial solution of the discrete variational equation*

$$U_{n+1} = G_u(u_n, \delta_0)U_n, \quad n \in \mathbb{Z}\,. \tag{3.7}$$

Then, system (3.1) *has a tangential homoclinic orbit $x_{\mathbb{Z}} \in S^N_{\mathbb{Z}}$ at $\alpha = \alpha_0 := K(\delta_0)$, which is explicitly given by*

$$x_i := H(u_i, \delta_0), \quad i \in \mathbb{Z}\,. \tag{3.8}$$

Furthermore, the sequence $X_{\mathbb{Z}} \in S^N_{\mathbb{Z}}$ defined as

$$X_i := H_u(u_i, \delta_0)U_i, \quad i \in \mathbb{Z} \tag{3.9}$$

satisfies the variational equation

$$X_{n+1} = f_x(x_n, \alpha_0)X_n, \quad n \in \mathbb{Z}\,. \tag{3.10}$$

Proof. Let us begin by showing that $x_{\mathbb{Z}}$ is a homoclinic orbit of (3.1). We then must first verify that $x_{\mathbb{Z}}$ is an orbit of (3.1). For this purpose, let $n \in \mathbb{Z}$ arbitrary. It follows

$$x_{n+1} = H(u_{n+1}, \delta_0) = H(G(u_n, \delta_0), \delta_0).$$

By taking into account the homological equation, we arrive at

$$x_{n+1} = H(G(u_n, \delta_0), \delta_0) = f(H(u_n, \delta_0), K(\delta_0)) = f(x_n, \alpha_0),$$

hence $x_{\mathbb{Z}}$ is indeed an orbit of (3.1). Now we will see that this orbit is homoclinic. Note that

$$\lim_{n\to\pm\infty} u_n = u_{eq},$$

where $u_{eq} \in \Omega_H$ is an equilibrium of the normal form. Consequently, we have that

$$\lim_{n\to\pm\infty} x_n = \lim_{n\to\pm\infty} H(u_n, \delta_0) = H(u_{eq}, \delta_0) =: x_{eq} \in \Omega_f.$$

Thus, it remains to show that x_{eq} is an equilibrium of (3.1). By the homological equation, it follows

$$f(x_{eq}, \alpha_0) = f(H(u_{eq}, \delta_0), K(\delta_0)) = H(G(u_{eq}, \delta_0), \delta_0) = H(u_{eq}, \delta_0) = x_{eq}.$$

Therefore, $x_{\mathbb{Z}}$ is a homoclinic orbit of (3.1). Now we have to show that $x_{\mathbb{Z}}$ is tangential, which amounts to proving that $X_{\mathbb{Z}}$ satisfies (3.10). To achieve this, we need the following relation

$$f_x(H(u,\delta),K(\delta))H_u(u,\delta) = H_u(G(u,\delta),\delta)G_u(u,\delta), \tag{3.11}$$

$(u,\delta) \in \Omega_H \times \Lambda_H$, which is obtained by differentiating with respect to u of the homological equation. Let $n \in \mathbb{Z}$ arbitrary. We have that

$$X_{n+1} = H_u(u_{n+1},\delta_0)U_{n+1} = H_u(G(u_n,\delta_0),\delta_0)U_{n+1}.$$

By combining (3.7) and (3.11), it follows:

$$\begin{aligned} X_{n+1} &= H_u(G(u_n,\delta_0),\delta_0)U_{n+1}, \\ &= H_u(G(u_n,\delta_0),\delta_0)G_u(u_n,\delta_0)U_n, \\ &= f_x(H(u_n,\delta_0),K(\delta_0))H_u(u_n,\delta_0)U_n, \\ &= f_x(x_n,\alpha_0)X_n. \square \end{aligned}$$

4 Flow Approximation

In the past section, the homological equation played the central role both in the center manifold reduction, as well as in the transformation of homoclinic orbits of the normal form to homoclinic orbits of the original system (3.1). In fact, Proposition 3.1 provides us formulae (3.8), (3.9), which allow the construction of tangential homoclinic orbits of system (3.1), provided a tangential homoclinic orbit of the normal form is available. In numerical applications we will of course be only able to approximate the homoclinic orbits of the original system, since the center manifold and the parameter transformation are only known up to a certain order. In other words, the problem of obtaining a first approximation of a tangential homoclinic orbit of an arbitrary N-dimensional system has been translated into approximating such orbits, but of the normal form, i.e., the dimension of the problem has been reduced.

In this section our efforts will be then dedicated to approximating tangential homoclinic orbits of the normal form of the $1:1$ resonance. For this purpose Lemma 2.5 will be of a great help, since it allows us to approximate the normal form by the 1-flow of a vector field (see Section 2), i.e., we transform the discrete-time problem into a continuous one. The advantage of doing so is that the dynamics of the approximating vector field is described by the well-known Bogdanov-Takens theory, and, in particular, the starting procedure for the continuation of homoclinic orbits near a Bogdanov-Takens point is available (cf. [3] and algorithms below). It would remain to know how to actually construct an approximating, discrete, tangential homoclinic orbit from a homoclinic orbit of the vector field. Once this construction is done, our starting procedure will be ready for numerical implementation.

Let $\phi^t(\cdot,\delta)$ be the t-flow of

$$\dot{u}(t) = g(u(t),\delta), \tag{4.1}$$

where g is the vector field given by Lemma 2.5. Then, according to this lemma, the discrete system

$$u \mapsto \psi(u,\delta) := \phi^1(u,\delta) \tag{4.2}$$

is an approximation of the normal form of the $1:1$ resonance. Suppose that system (4.1) has a homoclinic orbit at $\delta = \delta_0 \in \mathbb{R}^2$, and let $u_0 \in \mathbb{R}^2$ be a point on this homoclinic orbit, so that u_0 is not an equilibrium. Let $u_{\mathbb{Z}} \in S^2_{\mathbb{Z}}$ be given by

$$u_i := \phi^i(u_0,\delta_0), \quad i \in \mathbb{Z}\,.$$

Then, it immediately follows that $u_{\mathbb{Z}}$ is a homoclinic orbit of system (4.2), and consequently, by Lemma 2.5, $u_{\mathbb{Z}}$ is an approximation of a homoclinic orbit of the normal form. Thus, it is left to construct a solution of the variational equation of (4.2) along the orbit $u_{\mathbb{Z}}$. Let $U_{\mathbb{Z}} \in S^2_{\mathbb{Z}}$ be given by

$$U_i := g(u_i,\delta_0), \quad i \in \mathbb{Z}\,.$$

Choose an arbitrary $n \in \mathbb{Z}$. Then, it follows that:

$$\begin{aligned}
U_{n+1} &= g(u_{n+1},\delta_0),\\
&= g(\phi^{n+1}(u_0,\delta_0),\delta_0),\\
&= \frac{d}{dt}\left(\phi^{t+1}(u_0,\delta_0)\right)_{t=n},\\
&= \frac{d}{dt}\left(\psi(\phi^{t}(u_0,\delta_0),\delta_0)\right)_{t=n},\\
&= \psi_u(u_n,\delta_0)\frac{d}{dt}\left(\phi^{t}(u_0,\delta_0)\right)_{t=n},\\
&= \psi_u(u_n,\delta_0)g(\phi^{n}(u_0,\delta_0),\delta_0),\\
&= \psi_u(u_n,\delta_0)U_n.
\end{aligned}$$

Therefore, we have that $U_{\mathbb{Z}}$ is indeed a solution of the variational equation of (4.2) along the homoclinic orbit $u_{\mathbb{Z}}$. With these computations we are ready to implement the starting procedure for the continuation of homoclinic tangencies near an $\mathrm{R1}_2$ point. The precise implementation of the starting method is summarized in the following Algorithm:

Starting procedure for homoclinic tangencies near an $\mathbf{R1}_2$ point

Let system (2.4) have an $\mathrm{R1}_2$ point at the origin. Let

$$A := \begin{pmatrix} g^0_x - I_N & b \\ c^T & 0 \end{pmatrix} \in \mathbb{R}^{N+1,N+1},$$

where $b, c \in \mathbb{R}^N$ are chosen in such a way that A is nonsingular. Compute $v_0, v_1, p_0, p_1 \in \mathbb{R}^N$ from the systems:

$$\begin{aligned}
A\begin{pmatrix} v_0 \\ l \end{pmatrix} &= \begin{pmatrix} 0 \\ 1 \end{pmatrix}, \qquad A\begin{pmatrix} v_1 \\ h \end{pmatrix} = \begin{pmatrix} v_0 \\ 0 \end{pmatrix},\\
A^T\begin{pmatrix} p_0 \\ l \end{pmatrix} &= \begin{pmatrix} 0 \\ 1 \end{pmatrix}, \qquad A^T\begin{pmatrix} p_1 \\ h \end{pmatrix} = \begin{pmatrix} p_0 \\ 0 \end{pmatrix}.
\end{aligned}$$

Normalize

$$\gamma := p_0^T v_1, \quad p_1 := \frac{1}{\gamma}\left(p_1 - \frac{1}{\gamma}(p_1^T v_1)p_0\right), \quad p_0 := \frac{1}{\gamma}p_0.$$

(i) **Linear transformations**

$$\begin{aligned}\begin{pmatrix} \beta_1 & \beta_2 \end{pmatrix} &:= p_0^T g_\alpha^0,\\ K_1 &:= \frac{1}{\beta_1^2+\beta_2^2}\begin{pmatrix} \beta_1 & \sigma\beta_2 \\ \beta_2 & -\sigma\beta_1 \end{pmatrix}, \quad \sigma \in \{-1,1\},\\ C &:= \begin{pmatrix} v_1 & 0 \end{pmatrix} - g_\alpha^0 K_1 \in \mathbb{R}^{N,2}.\end{aligned}$$

Solve the two linear systems

$$A\begin{pmatrix} D \\ h \end{pmatrix} = \begin{pmatrix} C \\ 0 \end{pmatrix}.$$

Let

$$\begin{aligned}\widetilde{K}(\delta) &:= K_1\delta,\\ \widetilde{H}(u,\delta) &:= \begin{pmatrix} v_0 & v_1 \end{pmatrix} u + D\delta.\end{aligned}$$

(ii) **Quadratic coefficients of the normal form**

It assumed that g_x can be evaluated explicitly. Choose a suitable $s > 0$ for numerical differentiation. Compute:

$$\begin{aligned}a &:= \frac{1}{2}s^{-1}p_0^T(g_x(sv_0,0) - g_x^0)v_0,\\ b &:= s^{-1}p_1^T(g_x(sv_0,0) - g_x^0)v_0 + s^{-1}p_0^T(g_x(sv_0,0) - g_x^0)v_1.\end{aligned}$$

(iii) **Flow approximation**

Let

$$\dot{\xi} = F(\xi,\nu), \tag{4.3}$$

with $F(\xi,\nu) := F_0(\nu) + F_1(\xi,\nu) + F_2(\xi)$, where:

$$F_0(\nu) := \begin{pmatrix} -\frac{1}{2}\nu_1 \\ \nu_1 \end{pmatrix},$$

$$F_1(\xi,\nu) := \begin{pmatrix} \xi_2 + \left(\frac{1}{3}b - \frac{1}{2}a\right)\nu_1\xi_1 + \left(\left(\frac{1}{5}a - \frac{5}{12}b\right)\nu_1 - \frac{1}{2}\nu_2\right)\xi_2 \\ \left(\frac{2}{3}a - \frac{1}{2}b\right)\nu_1\xi_1 + \left(\left(\frac{1}{2}b - \frac{1}{6}a\right)\nu_1 + \nu_2\right)\xi_2 \end{pmatrix},$$

and

$$F_2(\xi) := \begin{pmatrix} -\frac{1}{2}a\xi_1^2 + \left(\frac{2}{3}a - \frac{1}{2}b\right)\xi_1\xi_2 + \left(\frac{1}{3}b - \frac{1}{6}a\right)\xi_2^2 \\ a\xi_1^2 + (b-a)\xi_1\xi_2 + \left(\frac{1}{6}a - \frac{1}{2}b\right)\xi_2^2 \end{pmatrix}.$$

Let $\xi_c(t)$, ν_c be the final approximation obtained in Step (iv) of the starting procedure for homoclinic orbits near a Bogdanov-Takens point (see algorithm below).

(iv) **Approximation of the homoclinic tangency of the normal form**

Choose $N_+, N_- \in \mathbb{Z}$, $N_- < 0 < N_+$, with $-N_-, N_+$ sufficiently large. Define the discrete interval $J := [N_-, N_+] \cap \mathbb{Z}$. Compute $u_J^d, U_J^d \in S_J^2$:

$$\begin{aligned} u_i^d &:= \xi_c(i), \\ U_i^d &:= F(u_i^d, \nu_c), \end{aligned}$$

$i \in J$.

(v) **Transformation of the homoclinic orbit of the normal form to the original system**

Compute $x_J^d, X_J^d \in S_J^N$, $\alpha_d \in \mathbb{R}^2$:

$$\begin{aligned} x_i^d &:= \widetilde{H}(u_i^d, \nu_c), \\ X_i^d &:= \widetilde{H}_u(u_i^d, \nu_c) U_i^d, \\ \alpha_d &:= \widetilde{K}(\nu_c), \end{aligned}$$

$i \in J$. Normalize

$$X_J^d := \frac{1}{\sqrt{\sum_{i=N_-}^{N_+} ||X_i^d||^2}} X_J^d.$$

Starting procedure for homoclinic orbits near a Bogdanov-Takens point

Let system

$$\dot{x}(t) = f(x(t), \alpha), \tag{4.4}$$

with $f : \mathbb{R}^N \times \mathbb{R}^2 \to \mathbb{R}^N$ sufficiently smooth, have a Bogdanov-Takens point at the origin. Let

$$A := \begin{pmatrix} f_x^0 & b \\ c^T & 0 \end{pmatrix} \in \mathbb{R}^{N+1,N+1},$$

where $b, c \in \mathbb{R}^N$ are chosen in such a way that A is nonsingular. Compute $v_0, v_1, p_0, p_1 \in \mathbb{R}^N$ from the systems:

$$\begin{aligned} A \begin{pmatrix} v_0 \\ g \end{pmatrix} &= \begin{pmatrix} 0 \\ 1 \end{pmatrix}, & A \begin{pmatrix} v_1 \\ h \end{pmatrix} &= \begin{pmatrix} v_0 \\ 0 \end{pmatrix}, \\ A^T \begin{pmatrix} p_0 \\ g \end{pmatrix} &= \begin{pmatrix} 0 \\ 1 \end{pmatrix}, & A^T \begin{pmatrix} p_1 \\ h \end{pmatrix} &= \begin{pmatrix} p_0 \\ 0 \end{pmatrix}. \end{aligned}$$

Normalize

$$\gamma := p_0^T v_1, \quad p_1 := \frac{1}{\gamma}\left(p_1 - \frac{1}{\gamma}(p_1^T v_1)p_0\right), \quad p_0 := \frac{1}{\gamma}p_0.$$

(i) **Linear transformations**

$$\begin{aligned} \begin{pmatrix} \beta_1 & \beta_2 \end{pmatrix} &:= p_0^T f_\alpha^0, \\ K_1 &:= \frac{1}{\beta_1^2 + \beta_2^2} \begin{pmatrix} \beta_1 & \sigma\beta_2 \\ \beta_2 & -\sigma\beta_1 \end{pmatrix}, \quad \sigma \in \{-1, 1\}, \\ C &:= \begin{pmatrix} v_1 & 0 \end{pmatrix} - f_\alpha^0 K_1 \in \mathbb{R}^{N,2}. \end{aligned}$$

Solve the two linear systems

$$A \begin{pmatrix} D \\ h \end{pmatrix} = \begin{pmatrix} C \\ 0 \end{pmatrix}.$$

Let $d_2 \in \mathbb{R}^{N+2}$ be the second column of $\begin{pmatrix} D \\ K_1 \end{pmatrix}$.

(ii) **Quadratic coefficients of the reduced system**

It is assumed that $f_z = \begin{pmatrix} f_x & f_\alpha \end{pmatrix}$, $z := (x, \alpha)$ can be evaluated explicitly. Choose a suitable $s > 0$ for numerical differentiation. Compute:

$$\begin{aligned} w_1 &:= s^{-1}(f_x(sv_0, 0) - f_x^0)v_0, & Q_{111} &:= p_1^T w_1, \\ w_4 &:= s^{-1}(f_z(sv_0, 0) - f_z^0)d_2, & Q_{211} &:= p_0^T w_1, \\ Q_{212} &:= s^{-1}p_0^T(f_x(sv_0, 0) - f_x^0)v_1, & Q_{214} &:= p_0^T w_4, \\ Q_{224} &:= s^{-1}p_0^T(f_x((0,0) + sd_2) - f_x^0)v_1, & Q_{114} &:= p_1^T w_4, \\ Q_{244} &:= s^{-1}p_0^T(f_z((0,0) + sd_2) - f_z^0)d_2. \end{aligned}$$

(iii) **Approximation of the homoclinic orbit of the reduced system**

$$\begin{aligned}
\Delta &:= Q_{211}(Q_{114}+Q_{224}) - Q_{214}(Q_{111}+Q_{212}),\\
\tau &:= \frac{5}{7\Delta}(Q_{111}+Q_{212}),\\
\sigma &:= \frac{1}{2Q_{211}}((Q_{114}^2 - Q_{211}Q_{244})\tau^2 - 1).
\end{aligned}$$

Choose a suitable $\epsilon > 0$ and let:

$$\begin{aligned}
\delta_1 &:= \sigma\epsilon^4,\\
\delta_2 &:= \tau\epsilon^2,\\
u_1(t) &:= \frac{\epsilon^2}{Q_{211}}\left(1 - 3\ \mathrm{sech}^2\left(\frac{\epsilon}{2}t\right) - Q_{214}\tau\right),\\
u_2(t) &:= \frac{3\epsilon^3}{Q_{211}}\ \mathrm{sech}^2\left(\frac{\epsilon}{2}t\right)\tanh\left(\frac{\epsilon}{2}t\right).
\end{aligned}$$

(iv) **Transformation of the homoclinic orbit of the reduced system to the original system**

$$\begin{aligned}
x(t) &:= \begin{pmatrix} v_0 & v_1 \end{pmatrix} u(t) + D\delta,\\
\alpha &:= K_1\delta.
\end{aligned}$$

5 Numerical Applications

We conclude this article with some numerical experiments whose purpose is to illustrate the use of the starting procedure. In what follows, after applying the starting procedure to the systems, we employ the thus obtained approximations for initializing (damped) Newton iterations of the defining systems given in terms of $\hat{\Upsilon}^T$, $\hat{\Upsilon}^P$ (cf. Section 2). Therefore, it is worth showing how the underlying matrices look like in order to implement the Newton iterations. These matrices will be denoted by A_T, A_P, respectively. Under notation of Section 2, let $M := |N_-|+N_++1$. The matrix A_T evaluated at $(x_J, u_J, \alpha) \in S_J^N \times S_J^N \times \mathbb{R}^2$ presents the following sparse structure

$$A_T := (a_{ij})_{i,j=1,\ldots,2NM+1} := \begin{pmatrix} & A_1 & & 0 & A_3\\ & & & 0 & 0\\ A_2 & 0 & & A_1 & A_4\\ 0 & 0 & & & 0\\ 0 & 0 & A_5 & & 0 \end{pmatrix}, \tag{5.1}$$

where:

$$
\begin{aligned}
(a_{ij})_{i=1,\dots,NM,j=1,\dots,NM} &:= A_1 \in \mathbb{R}^{NM,NM},\\
(a_{ij})_{i=NM+1,\dots,2NM,j=NM+1,\dots,2NM} &:= A_1,\\
(a_{ij})_{i=NM+1,\dots,N(2M-1),j=1,\dots,N(M-1)} &:= A_2 \in \mathbb{R}^{N(M-1),N(M-1)},\\
(a_{ij})_{i=1,\dots,N(M-1),j=2NM+1} &:= A_3 \in \mathbb{R}^{N(M-1)},\\
(a_{ij})_{i=NM+1,\dots,N(2M-1),j=2NM+1} &:= A_4 \in \mathbb{R}^{N(M-1)},\\
(a_{ij})_{i=2NM+1,j=NM+1,\dots,2NM} &:= A_5 \in \mathbb{R}^{1,NM},
\end{aligned}
$$

and

$$
A_1 := \begin{pmatrix}
-f_x(x_{N_-},\alpha) & I_N & & & 0\\
& \ddots & \ddots & & \\
0 & & \ddots & \ddots & \\
& & -f_x(x_{N_+-1},\alpha) & & I_N\\
I_N & & 0 & & -I_N
\end{pmatrix},
$$

$$
A_2 := \begin{pmatrix}
-f_{xx}(x_{N_-},\alpha)[u_{x_{N_-}}] & & & & 0\\
& \ddots & & & \\
& & \ddots & & \\
0 & & & & -f_{xx}(x_{N_+-1},\alpha)[u_{x_{N_+-1}}]
\end{pmatrix},
$$

$$
A_3 := \begin{pmatrix}
-f_{\alpha_1}(x_{N_-},\alpha)\\
\vdots\\
-f_{\alpha_1}(x_{N_+-1},\alpha)
\end{pmatrix},
$$

$$
A_4 := \begin{pmatrix}
-f_{x\alpha_1}(x_{N_-},\alpha)u_{x_{N_-}}\\
\vdots\\
-f_{x\alpha_1}(x_{N_+-1},\alpha)u_{x_{N_+-1}}
\end{pmatrix},
$$

$$
A_5^T := 2\begin{pmatrix}
u_{x_{N_-}}\\
\vdots\\
u_{x_{N_+}}
\end{pmatrix},
$$

where $f_{xx}(x,\alpha)[u] := (f_x(x,\alpha)u)_x$, $(x,u,\alpha) \in \mathbb{R}^N \times \mathbb{R}^N \times \mathbb{R}^2$. Moreover, the matrix A_P is computed similarly as A_T. Just the rows of A_p that are related to the boundary conditions differ from those of A_T, as the projection boundary conditions have a different structure and furthermore they depend on the parameter α, in contrast to the periodic ones.

Once we have found a homoclinic tangency, continuation with respect to a second parameter, say α_2, is possible. By doing so, we will obtain an approximation of a first curve of homoclinic tangencies that emanates from the $\mathrm{R1}_2$ point. On the other hand, continuation with respect to one parameter, with the other one fixed, will allow us to obtain a closed curve of transversal homoclinic orbits. In this way, a second homoclinic tangency can be found, and thereby a second curve of homoclinic tangencies can be

continued. For the purposes above described, we will use the Euler-Newton method (cf. [1, Algorithm 10.2.10]) combined with step-size control as described in [10, Section 2.3].

Although the starting procedure for homoclinic tangencies is essentially a theory-based method, there is still a trial-and-error-component which cannot be avoided. This component is found in the choice of a "suitable" $\epsilon > 0$ in Step (iii) of the starting method for homoclinic orbits near a Bogdanov-Takens point (see Section 4). It is clear that the smaller ϵ is chosen, the better is the approximation of the homoclinic orbit, however, also the worse is the condition of the defining system whose solution we need to find. Therefore, there exists a compromise between approximation of the homoclinic orbit and conditioning of the underlying system. Roughly speaking, we can visualize this compromise as if there existed an interval $(\epsilon_{min}, \epsilon_{max})$, $0 < \epsilon_{min} < \epsilon_{max}$, in which we should try choosing values of ϵ in order to generate a converging, nontrivial sequence via (damped) Newton iterations. Choosing values of ϵ outside this interval will be likely to produce either diverging sequences or trivial solutions (i.e. sequences of equilibria, or more complicated types of spurious solutions, etc.).

Throughout the numerical applications, $||\cdot||$ will represent the Euclidean norm. Moreover, for the continuation of transversal homoclinic orbits, we use the amplitude function

$$\mathrm{ampl}(x_J, \alpha) := \sqrt{\sum_{i=N_-}^{N_f} ||x_i - \xi(\alpha)||^2},$$

where $N_f := N_+$ (resp. $N_f := N_+ - 1$), if we use projection boundary conditions (resp. periodic boundary conditions), and $\xi(\alpha)$ stands for the parameter-dependent equilibrium which the points of the homoclinic orbit converge to. This function will allow us to visualize closed curves of transversal homoclinic orbits.

In all the numerical examples we will first compute a tangential homoclinic orbit x_J^0 with $-N_- = N_+ = 20$. Then, if an orbit with a larger length is desired, we set an initial approximating orbit to

$$(\ldots, \xi, \ldots, \xi, x_J^0, \xi, \ldots, \xi, \ldots),$$

and then we use it for the corresponding Newton iterations.

Finally, all the computations will be performed with MATLAB.

5.1 Normal form of the $1:1$ resonance

Consider the system

$$\begin{pmatrix} x_1 \\ x_2 \end{pmatrix} \mapsto g(x, \alpha) := \begin{pmatrix} x_1 + x_2 \\ x_2 + \alpha_1 + \alpha_2 x_2 + x_1^2 + x_1 x_2 \end{pmatrix}, \tag{5.2}$$

where $x := (x_1, x_2) \in \mathbb{R}^2$, $\alpha := (\alpha_1, \alpha_2) \in \mathbb{R}^2$. This system was already discussed in Section 2. Let us apply the starting procedure to (5.2). The matrix A is given by

$$A := \begin{pmatrix} 0 & 1 & 1 \\ 0 & 0 & 1 \\ 1 & 1 & 0 \end{pmatrix}.$$

By means of this matrix we obtain the linear transformations:

$$\widetilde{K}(\delta) := \begin{pmatrix} 1 & 0 \\ 0 & 1 \end{pmatrix} \delta,$$
$$\widetilde{H}(u,\delta) := \begin{pmatrix} 1 & -1 \\ 0 & 1 \end{pmatrix} u + \begin{pmatrix} 1 & 0 \\ -1 & 0 \end{pmatrix} \delta.$$

The computed quadratic coefficients are:

$$a := 1, \quad b := 1.$$

With these coefficients we obtain the following ϵ-dependent flow approximation:

$$\begin{aligned} \delta_1 &:= -\tfrac{1}{4}\epsilon^4, \\ \delta_2 &:= -0.35714285714052\epsilon^2, \\ u_1(t) &:= \tfrac{\epsilon^2}{2}\left(1 - 3\ \mathrm{sech}^2\left(\tfrac{\epsilon}{2}t\right)\right), \\ u_2(t) &:= \tfrac{3\epsilon^3}{2}\ \mathrm{sech}^2\left(\tfrac{\epsilon}{2}t\right)\tanh\left(\tfrac{\epsilon}{2}t\right) + \tfrac{1}{2}\delta_1. \end{aligned} \tag{5.3}$$

It is important to point out that this step can be easily automatized, since the critical eigenvectors of the approximating vector field do not depend on a, b. Therefore, only the Q's (cf. Step (ii) of the starting method near Bogdanov-Takens points) must be recomputed in each example.

By choosing $\epsilon := 0.9$, $N_- := -40$, $N_+ := 60$, and after some damped Newton iterations, we find a homoclinic tangency x_J, X_J at

$$(\alpha_1, \alpha_2) = (-0.2135818065347, -0.28928571428382),$$

with

$$||\hat{\Upsilon}^T(x_J, X_J, \alpha)|| \approx 8.33 \times 10^{-12}.$$

In order to verify that the so obtained orbit x_J is actually a homoclinic tangency, we plot the stable and unstable manifolds of the system. These are shown in Figure 5.1 and 5.2. In these pictures we can see that the points of x_J indeed correspond to the tangential intersections of W^u_ξ and W^s_ξ. These manifolds are approximated via forward (resp. backward) iterations of (5.2) starting from points on the tangent space of W^u_ξ (resp. W^s_ξ) at ξ, close enough to the equilibrium.

The next experiment will be the continuation of transversal homoclinic orbits with respect to α_1, letting $\alpha_2 = -0.28928571428382$ fixed. The result is shown in Figure 5.3. In this picture we obtained a closed loop, which is a known phenomenon that is a consequence of the behavior of the stable and unstable manifolds under perturbation (cf. [6]). Along this curve we marked the points P_{T_1}, P_{T_r}, and P_{T_2}, which correspond to the first homoclinic tangency (i.e. the one we have already computed), a transversal homoclinic point, and a second homoclinic tangency, respectively. The transversal homoclinic orbit is located at

$$(\alpha_1, \alpha_2) = (-0.21528248893748, -0.28928571428382).$$

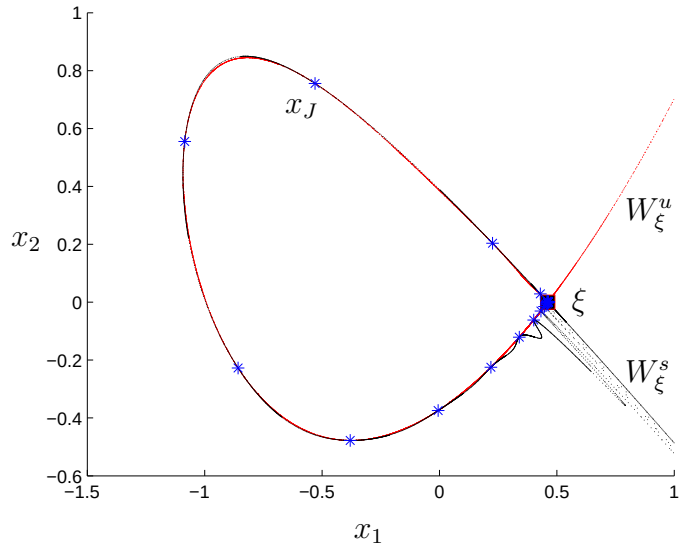

Fig. 5.1: Stable and unstable manifolds along the homoclinic tangency x_J.

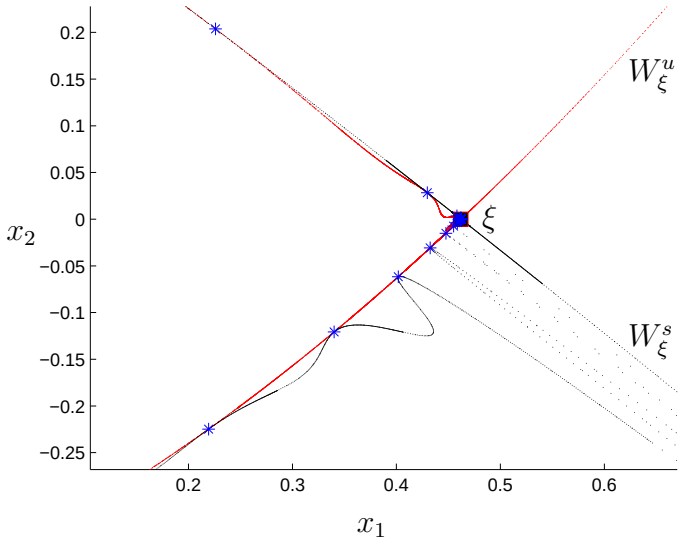

Fig. 5.2: Stable and unstable manifolds around the equilibrium ξ.

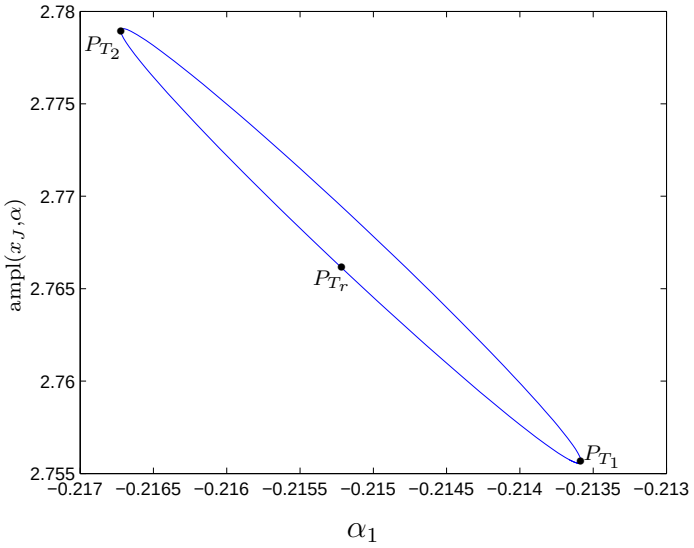

Fig. 5.3: Continuation of transversal homoclinic orbits with respect to α_1, with α_2 fixed.

Furthermore, in Figure 5.4, we show the transversal intersections of the manifolds along the homoclinic orbit. Now we will switch to the second homoclinic tangency. To achieve this, we first use P_{T_2} as a starting point for the Newton iterations. This point is, in parameter space, located at

$$(\alpha_1, \alpha_2) = (-0.21672274959574, -0.28928571428382).$$

In this way, we obtain a very good approximation of both the parameter values, as well as of the second tangential homoclinic orbit, which will be denoted by y_J^0. However, we also need an initial value Y_J^0 for the solution of the variational equation of (5.2) along y_J^0. In order to construct Y_J^0, we use the fact that the matrix

$$\hat{\Gamma}^T_{x_J}(y_J^0, \alpha)$$

is almost singular, which allows us to find a vector Y_J^0, such that

$$\hat{\Gamma}^T_{x_J}(y_J^0, \alpha) Y_J^0 \approx 0.$$

This step can be easily implemented by a single command in MATLAB. Thus, after some few Newton iterations, we found a second homoclinic tangency y_J, Y_J at

$$(\alpha_1, \alpha_2) = (-0.2167231774074, -0.28928571428382),$$

with

$$||\hat{\Upsilon}^T(y_J, Y_J, \alpha)|| \approx 5.93 \times 10^{-12}.$$

In Figure 5.5 we show the tangential intersections of the manifolds along the homoclinic orbit y_J.

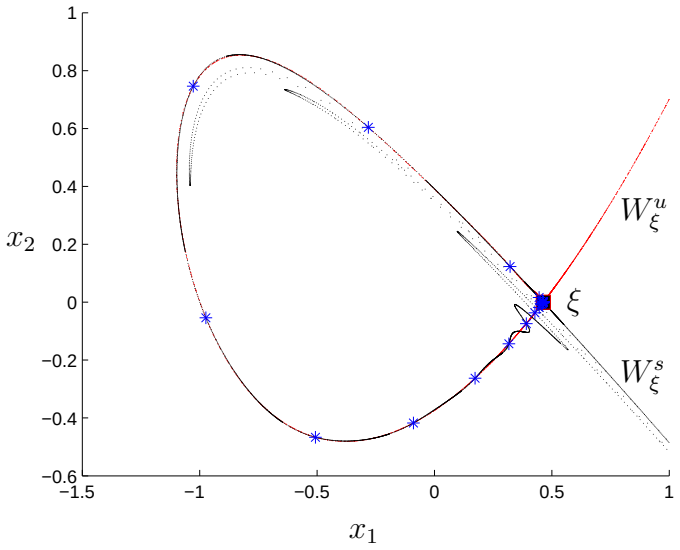

Fig. 5.4: Stable and unstable manifolds along a transversal homoclinic orbit.

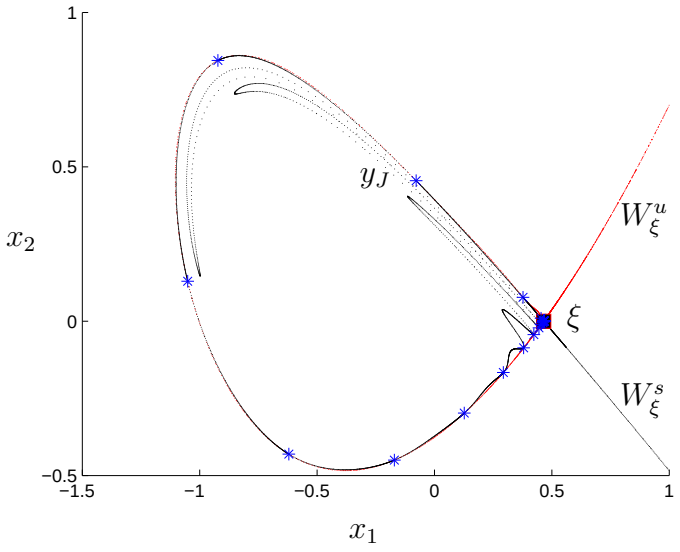

Fig. 5.5: Stable and unstable manifolds along the second homoclinic tangency y_J.

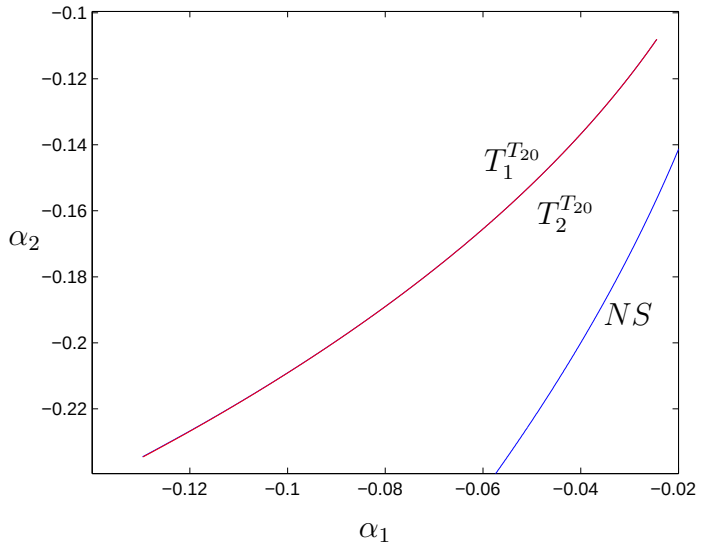

Fig. 5.6: Tangential homoclinic branches.

Our next goal in this experiment is to numerically compute the "horn" of homoclinic tangencies that emanates from the $\mathrm{R1}_2$ point. This horn consists of two branches of tangential homoclinic orbits, which are schematically shown in Figure 2.1. Note that in the above performed computations, we already obtained two points of the horn, namely, P_{T_1} and P_{T_2} (see Figure 5.3).

The experiment is performed as follows. Choose $\epsilon := 0.55$ in (5.3), $N_- := -20$, $N_+ := 20$ with the corresponding discrete interval J_{20}. With these values we obtain two homoclinic tangencies $x_{J_{20}}, X_{J_{20}}$, and $y_{J_{20}}, Y_{J_{20}}$, located at

$$\alpha_x = (-0.02442993556905, -0.10803571428571),$$

and

$$\alpha_y = (-0.02442993416031, -0.10803571428571),$$

respectively, with

$$||\hat{\Upsilon}^T(x_{J_{20}}, X_{J_{20}}, \alpha_x)|| \approx 2 \times 10^{-13}, \quad ||\hat{\Upsilon}^T(y_{J_{20}}, Y_{J_{20}}, \alpha_y)|| \approx 6.01 \times 10^{-12}.$$

With this information we are ready to perform the continuation of the horn. The result of the continuation is shown in Figure 5.6. The tangential homoclinic branches are labeled by $T_1^{T_{20}}$, $T_2^{T_{20}}$. The superscript T_{20} denotes the use of periodic boundary conditions within the interval J_{20} above defined. The label NS denotes the Neimark-Sacker curve. In Figure 5.6 we can observe that the position of the curves in the parameter space is consistent with Figure 2.1, however, the width of the horn is actually much smaller. In fact, we will next see how small this width really is. To achieve this, we perform the continuation of $T_1^{T_{20}}$, and then, for some α_2's fixed, we continue transversal homoclinic orbits with respect to α_1 (see Figure 5.3). The width of the horn is then obtained by measuring the difference

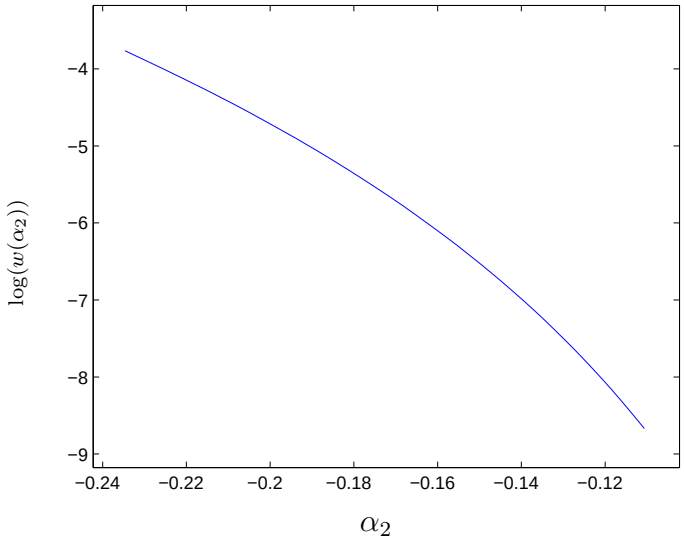

Fig. 5.7: Width of the homoclinic horn.

between the maximum and minimum values that α_1 attains along the closed curve of transversal homoclinic orbits. Of course, this procedure is not performed for every point of $T_1^{T_{20}}$, otherwise the numerical and time cost would have been unnecessarily high. The result of this process is shown in Figure 5.7. In this picture $w(\alpha_2)$ stands for the width of the horn with respect to α_2. It draws our attention how small the region between $T_1^{T_{20}}$ and $T_2^{T_{20}}$ really is, and furthermore, we can also observe that the width increases as the parameters move away from the $\mathrm{R1}_2$ point along $T_1^{T_{20}}$, which is consistent with the theory (cf. [8], [17, Section 9.5.2]).

5.2 Hénon 3D map

The Hénon map has proven to be very rich in terms of its bifurcation diagram and fascinating global phenomena that this system exhibits (cf. [17], [19]). In this experiment we consider the following three-dimensional version of the Hénon map

$$\begin{pmatrix} x \\ y \\ z \end{pmatrix} \mapsto \begin{pmatrix} \alpha_2 + \alpha_1 z - x^2 \\ x \\ y \end{pmatrix}.$$

This system undergoes an $\mathrm{R1}_2$ singularity at $(x, y, z) = (-0.75, -0.75, -0.75)$, $(\alpha_1, \alpha_2) = (-0.5, -0.5625)$. Next, we apply the starting procedure to the Hénon system, with $\epsilon := 0.9$, $N_- := -50$, $N_+ := 50$, and

$$A := \begin{pmatrix} 0.5 & 0 & -0.5 & 0.8 \\ 1 & -1 & 0 & -0.4 \\ 0 & 1 & -1 & -0.4 \\ 0.5 & 0.5 & 0.5 & 0 \end{pmatrix}.$$

After some few Newton iterations, we find a homoclinic tangency x_J, X_J at

$$(\alpha_1, \alpha_2) = (-1.14448083063938, -0.23373257142857),$$

with

$$||\hat{\Upsilon}^P(x_J, X_J, \alpha)|| \approx 8.12 \times 10^{-12}.$$

In Figure 5.8 and 5.9 we show the phase plot of the computed orbit x_J and the exponential decay of $||X_i||$, $i \in J$, respectively. It is interesting noting that the shape of the computed

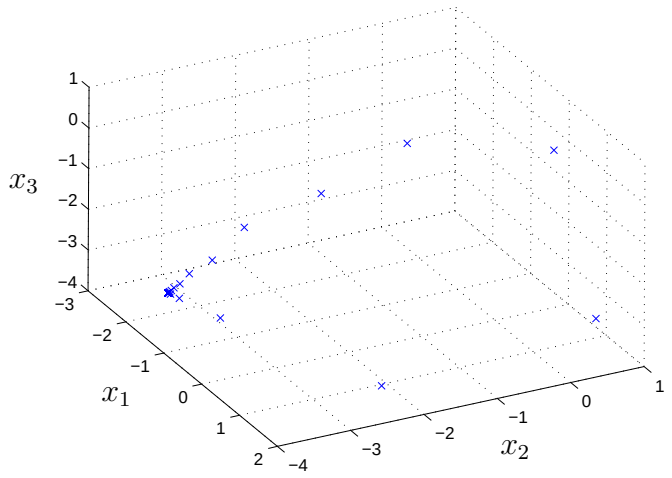

Fig. 5.8: Homoclinic orbit x_J.

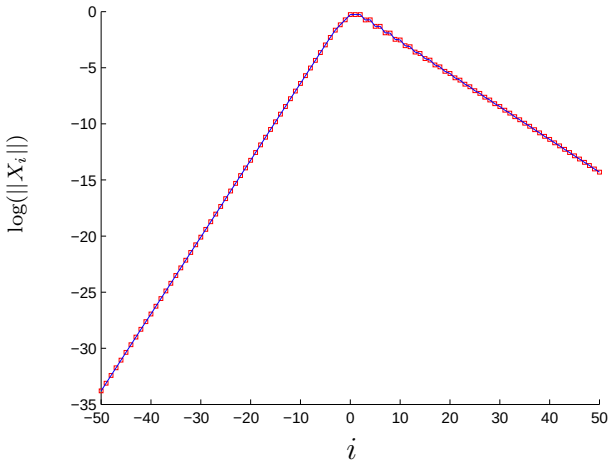

Fig. 5.9: Exponential decay of $||X_i||$ with respect to i.

homoclinic tangency x_J is similar to that of the homoclinic tangencies computed for

the normal form, see e.g. Figure 5.1. However, the very same Hénon map may exhibit homoclinic tangencies with a totally different shape, if we choose another suitable value of parameters (cf. [15, Section 7.1.3]).

Acknowledgements

The author is deeply indebted to Wolf-Jürgen Beyn and Thorsten Hüls for stimulating discussions and suggestions about the present work.

References

[1] Allgower, E., and Georg, K. *Introduction to Numerical Continuation Methods*, vol. 45 of *Classics in Applied Mathematics*. SIAM, New York, 2003.

[2] Arrowsmith, D., Cartwright, J., Lansbury, A., and Place, C. The Bogdanov Map: Bifurcations, Mode Locking, and Chaos in a Dissipative System. *Internat. J. of Bif. and Chaos 3*, 4 (1993), 803–842.

[3] Beyn, W.-J. Numerical analysis of homoclinic orbits emanating from a Takens-Bogdanov point. *IMA Journal of Numerical Analysis 14* (1994), 381–410.

[4] Beyn, W.-J., Champneys, A., Doedel, E., Govaerts, W., Kuznetsov, Y. A., and Sandstede, B. Numerical continuation, and computation of normal forms. In *Handbook of Dynamical Systems*, B. Fiedler, Ed., vol. 2. Elsevier, 2002, pp. 149–219.

[5] Beyn, W.-J., and Kleinkauf, J.-M. The numerical computation of homoclinic orbits for maps. *SIAM J. Numer. Anal. 34*, 3 (1997), 1207–1236.

[6] Beyn, W.-J., and Zou, J.-K. On manifolds of connecting orbits in discretizations of dynamical systems. *Nonlinear Anal. 52*, 5 (2003), 1499–1520.

[7] Beyn, W.-J., Zou, J.-K., Hüls, T., and Kleinkauf, J.-M. Numerical analysis of degenerate connecting orbits for maps. *Internat. J. of Bif. and Chaos 14*, 10 (2004), 3385–3407.

[8] Broer, H., Simó, C., and Roussarie, R. Invariant circles in the Bogdanov-Takens bifurcation for diffeomorphisms. *Ergod. Th. & Dynam. Sys. 16*, 6 (1996), 1147–1172.

[9] Chow, S.-N., Li, C., and Wang, D. *Normal Forms and Bifurcation of Planar Vector Fields*. Cambridge University Press, New York, 1994.

[10] Dhooge, A., Govaerts, W., Kuznetsov, Y. A., Mestrom, W., Riet, A. M., and Sautois, B. *MATCONT and CL_MATCONT: Continuation toolboxes in MATLAB*. University of Gent, Belgium, 2006. Available at `http://www.matcont.ugent.be/manual.pdf`.

[11] Govaerts, W., Kuznetsov, Y. A., Khoshsiar Ghaziani, R., and Meijer, H. G. E. Numerical methods for two-parameter local bifurcation analysis of maps. *SIAM J. Sci. Comput. 29*, 6 (2007), 2644–2667.

[12] Govaerts, W., Kuznetsov, Y. A., Khoshsiar Ghaziani, R., and Meijer, H. G. E. *Cl_MatContM: A toolbox for continuation and bifurcation of cycles of maps*. University of Gent, Belgium, 2008. Available at `http://sourceforge.net/projects/matcont/`.

[13] Kleinkauf, J.-M. The numerical computation and geometrical analysis of heteroclinic tangencies. Available at `http://www.mathematik.uni-bielefeld.de/sfb343/`. Preprint 98-48, SFB 343, University of Bielefeld, 1998.

[14] Kleinkauf, J.-M. Numerische Berechnung diskreter homokliner Orbits. Master's thesis, University of Bielefeld, Germany, 1994.

[15] Kleinkauf, J.-M. *Numerische Analyse tangentialer homokliner Orbits*. PhD thesis, University of Bielefeld, Germany, 1997.

[16] Kuznetsov, Y. A. Numerical Normalization Techniques for all codim 2 Bifurcations of Equilibria in ODE'S. *SIAM J. Numer. Anal. 36*, 4 (1999), 1104–1124.

[17] Kuznetsov, Y. A. *Elements of Applied Bifurcation Theory*, third ed., vol. 112 of *Applied Mathematical Sciences*. Springer-Verlag, New York, 2004.

[18] Kuznetsov, Y. A., Van Veen, L., and Meijer, H. G. E. The fold-flip bifurcation. *Internat. J. of Bif. and Chaos 14*, 7 (2004), 2253–2282.

[19] Meijer, H. G. E. *Codimension 2 Bifurcations of Iterated Maps*. PhD thesis, University of Utrecht, Netherlands, 2006.

[20] Páez Chávez, J. *Numerical Analysis of Dynamical Systems with Codimension two Singularities*. PhD thesis, Bielefeld University, Germany, 2009. Available at `http://bieson.ub.uni-bielefeld.de/volltexte/2009/1467/`.